energies

MDPI

Article

Enhancing Energy Sustainability in Remote Mining Operations Through Wind and Pumped-Hydro Storage; Application to Raglan Mine, Canada

Adrien Tardy, Daniel R. Rousse, Baby-Jean Robert Mungyeko Bisulandu and Adrian Ilinca *

Mechanical Engineering, T3E Research Group, École de Technologie Supérieure (ÉTS), Montréal, QC H3C 1K3, Canada; adrien.tardy.1@ens.etsmtl.ca (A.T.); daniel.rousse@etsmtl.ca (D.R.R.); baby-jeanrobert.mungyekobisulandu@etsmtl.ca (B.-J.R.M.B.)

* Correspondence: adrian.ilinca@etsmtl.ca

Abstract: The Raglan mining site in northern Quebec relies on diesel for electricity and heat generation, resulting in annual emissions of 105,500 tons of CO_2 equivalent. This study investigates the feasibility of decarbonizing the site's power generation system by integrating a renewable energy network of wind turbines and a pumped hydro storage plant (PHSP). It uniquely integrates PHSP modeling with a dynamic analysis of variable wind speeds and extreme climatic conditions, providing a novel perspective on the feasibility of renewable energy systems in remote northern regions. MATLAB R2024b-based simulations assessed the hybrid system's technical and economic performance. The proposed system, incorporating a wind farm and PHSP, reduces greenhouse gas (GHG) emissions by 50%, avoiding 68,500 tons of CO_2 equivalent annually, and lowers diesel consumption significantly. The total investment costs are estimated at 2080 CAD/kW for the wind farm and 3720 CAD/kW for the PHSP, with 17.3 CAD/MWh and 72.5 CAD/kW-year operational costs, respectively. The study demonstrates a renewable energy share of 52.2% in the energy mix, with a payback period of approximately 11 years and substantial long-term cost savings. These findings highlight the potential of hybrid renewable energy systems to decarbonize remote, off-grid industrial operations and provide a scalable framework for similar projects globally.

Keywords: decarbonization; wind turbines; renewable energies; wind farm; energy storage; PHSP

check for updates

Academic Editors: Frede Blaabjerg and Tek Tjing Lie

Received: 11 March 2025
Revised: 19 April 2025
Accepted: 22 April 2025
Published: 24 April 2025

Citation: Tardy, A.; Rousse, D.R.; Mungyeko Bisulandu, B.-J.R.; Ilinca, A. Enhancing Energy Sustainability in Remote Mining Operations Through Wind and Pumped-Hydro Storage; Application to Raglan Mine, Canada. *Energies* **2025**, *18*, 2184. https://doi.org/10.3390/en18092184

1. Introduction

As the world undergoes an ecological transition, countries that signed the Paris Agreement have committed to significantly reducing greenhouse gas (GHG) emissions by cutting the consumption of fossil fuels, which are known contributors to pollution. As a signatory, Canada accounted for 0.73 Gt CO_2 equivalent emissions in 2013 [1] and 0.69 Gt of CO_2 in 2023 [2], representing 1.95% and 1.2% of global GHG emissions, respectively. The country has set ambitious targets to reduce national GHG emissions by 40–45% by 2030 and achieve net-zero emissions by 2050 [3–6].

In this context, the Raglan mining company has prioritized decarbonizing its operations, focusing specifically on its electricity production system. Located in the remote Nunavik region of northern Quebec, the Raglan mining site primarily produces raw nickel through ore exploration, underground excavation, and rock separation. Due to its remote location, the mine is not connected to Quebec's public electricity grid, which is predominantly powered by hydroelectric energy (97%) [5]. Instead, Raglan operates its electricity production network, which includes thermal power stations and two 3 MW wind turbines. This network heavily relies on diesel, which has a significant environmental impact.

In 2021, the mine consumed 58.9 million liters of diesel, with electricity generation alone accounting for 73% of this consumption, resulting in 119,440 tons of CO_2 equivalent emissions. Self-propelled mining equipment accounted for the remaining 27%, emitting 44,400 tons of CO_2 equivalent. The site's 25 kV network (25 kV-G) operates on a cogeneration principle (see Figure 1), where six of its twenty generators (Electro-Motive Diesel, EMD generators in Figure 1) feature recovery loops that fulfill the mine's heating requirements, including ore drying, building heating, and domestic hot water.

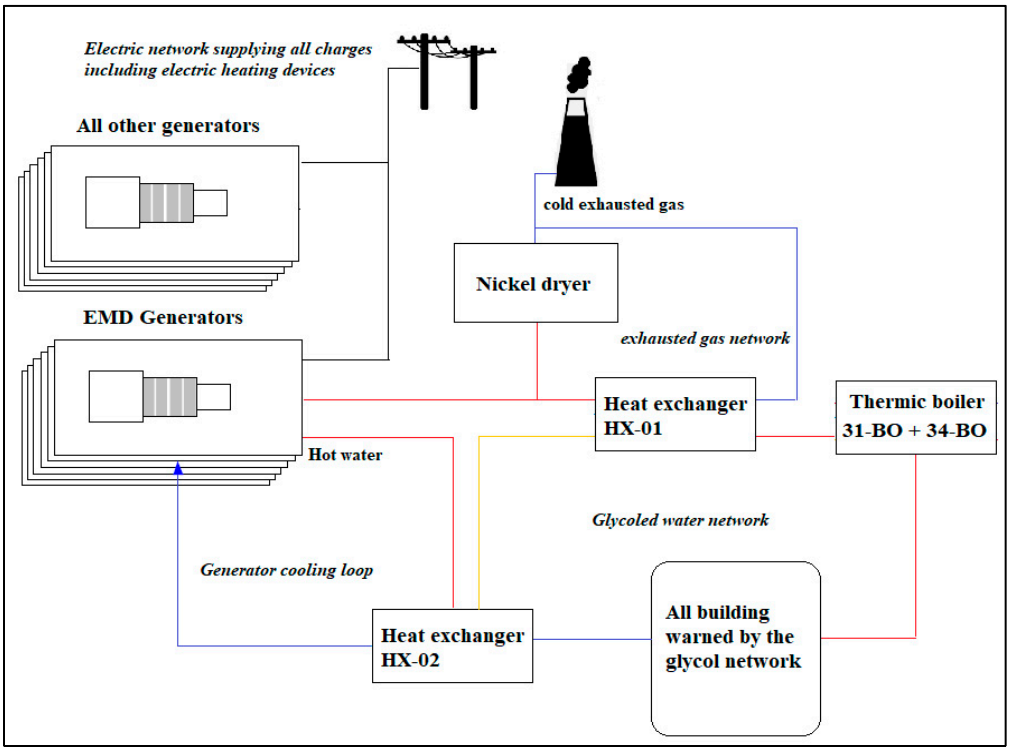

Figure 1. Scheme of the integrated electrical and heating networks.

Notably, Raglan is the first site in Canada's far north to successfully implement large wind turbines. Building on this achievement, the mine aims to expand its wind energy capacity with a larger wind farm, aligning with its environmental goals and reducing energy costs.

Green technologies in the electricity generation sector are now necessary in the context of limited energy resources and, above all, to reduce GHG emissions. Heavy industries are increasingly launching programs to decarbonize their facilities. Du et al. [7] emphasize the need for a profound transition in the electricity sector on a global scale to achieve decarbonization objectives. According to Balaban et al. [8], profound changes in the electricity production chain (transport, electricity consumption, etc.) are necessary to decarbonize an energy system, as two-thirds of total GHG emissions come from the electricity production sector. According to Dongsheng et al. [9], a resilient energy future by 2050 is only possible if sustainable and cost-effective energy solutions are considered in the power generation sector. Obiora et al. [10] and Roshan Kumar et al. [11] emphasize that decarbonization must be preceded by a transition to low-carbon energy infrastructures, which is the only way to mitigate the severe environmental impacts of climate change.

Significantly reducing the share of fossil fuels in the energy mix must be a major objective for any installation dedicated to electricity generation [12]. Wang et al. [13] highlight the importance of hydropower in achieving carbon neutrality. They believe that deep decarbonization can be achieved if considerable efforts are made and large-scale projects in the hydropower sector are initiated. Lee et al. [14] recommend using hydrogen, carbon capture and storage (CCS) technologies, and bioenergy as options for decarbonization in industry. Promising strategies for deep decarbonization depend exclusively on integrating renewable energies [15]. The first pumped hydro storage plant (pumped hydro storage plant, PHSP) appeared in Italy and Switzerland at the end of the 20th century and is now the most widely used large-scale storage system. With almost 160 GW and 9000 GWh installed worldwide, these plants represent over 90% of the total storage capacity [16]. The PHSP is the most advanced technique for stationary energy storage [17,18]. Pumped storage power (PSP) plants are energy sources that regulate renewable energy electricity networks (e.g., wind and photovoltaic) [19]. Figure 2 provides a schematic representation of a typical PHSP. An example of a pumped storage facility in Canada is Ontario Power Generation's Sir Adam Beck Pumped Storage Generating Station, which has a capacity of 174 megawatts. It pumps water from the Niagara River into a 300-hectare reservoir for energy storage [20].

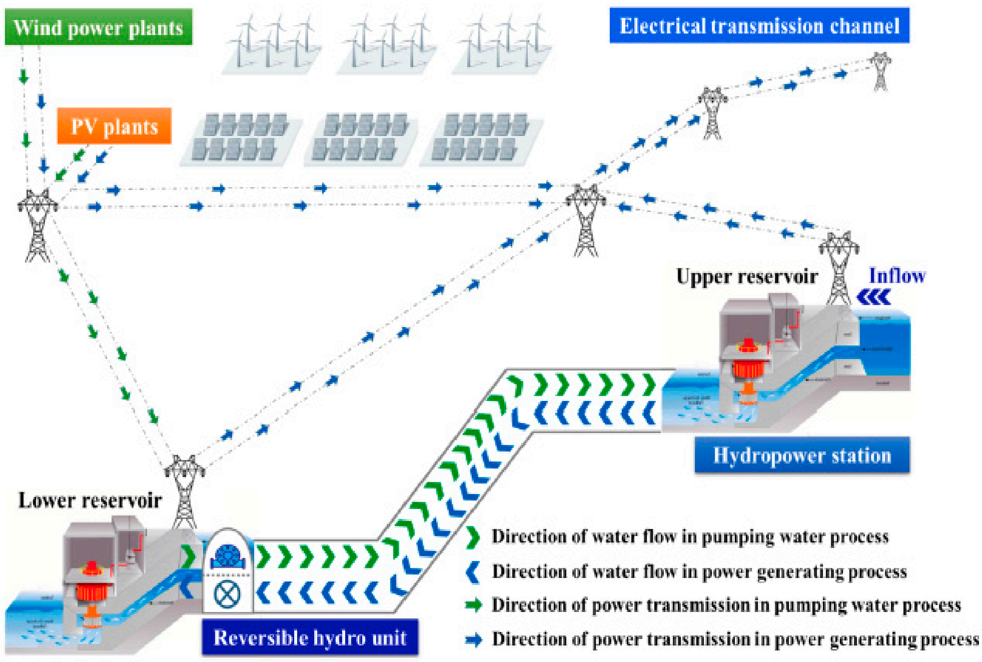

Figure 2. A multi-energy complementary power generation system of hydropower, wind power, and PV, including the hybrid pumped storage power station [19].

In this context, the pumped storage hydroelectric plant was chosen to store surplus energy from the local network because of its simplicity, technological maturity, regulation, and ability to secure the electricity network. It can be used to regulate peaks, reduce fluctuations in renewable energy sources, and optimize energy production by storing surplus energy [21–25]. Hence, this project aims to study the possibility of decarbonizing the Raglan Mine site's electricity production system (the 25 kV-G network) by significantly reducing or even eliminating diesel consumption by integrating a wind farm coupled with a PHSP.

The specific objectives are as follows:

- Provide an overview of the PHSP solution;
- Introduce the stochastic models;
- Formulate, implement, and validate a performance prediction method;

- Size the PHSP according to the power needed, topology, wind power capacity, required decarbonization level, and financial viability.

There are multiple advantages of PHSPs, making them particularly interesting for integrating fluctuating energies such as wind power. The works of the IHA [26,27] are conclusive and agree on the technology's assets, starting with analyzing the transitory periods and explaining that PHSPs' dynamic responses are fast and stable. This flexibility from hydro dams' energy allows for the best possible tracking of the grid's power demand. Secondly, besides having a high overall efficiency (70 to 85%), stationary generation offers mechanical inertia, which helps maintain the grid's frequency stability. Finally, due to the significant size of the water reservoirs and the power that can be installed, PHSPs can meet storage needs on a large scale and for various periods, ranging from several months to a few minutes.

Silva et al. [18] focused on the role of pumped storage hydropower in the context of energy storage in the event of an increase in renewable energy capacity. The results of this study show that it is possible to increase renewable energies to 85%, thanks to pumped hydroelectric storage, while reducing emissions by 1 Mton of CO_2 eq from electricity production. To increase the absorption of electricity from renewable energies into the power grid, Zhou et al. [28] proposed an optimization operation framework for a peak-shaving and valley-filling (PS-VF) operation-driven PHSP station located in Hunan Province, China. The authors argue that hydropower generation, CO_2 emission reduction, and power system stability are consequences of efficiently optimizing the pumped storage station. Zhou et al. [29] were interested in integrating renewable energies into the electricity grid while minimizing residual load fluctuations and adapting to the intermittent nature of renewable energies. To this end, they proposed the joint use of hydroelectric and off-river pumped storage power stations.

Wu et al. [30] provided a framework for planning and designing a pumped storage station in an integrated base. The study concerned a hydro-photovoltaic storage unit in Xizang province, with a total installed capacity of 49,485 MW. The results show that 89.86% of the power absorbed in the integrated base is controllable. This highlights the significant role of pumped storage in the high-quality development and high proportion of the integrated hydropower–wind–photovoltaic storage base.

To meet these needs, the first issue is to identify relevant sites for PHSPs. For this purpose, a powerful tool is presented in these works [31–34]. The Geographic Information System (GIS) is a mathematical model that scans the topography of an area by adopting selection criteria with a weighting system for these criteria. This tool allows the listing and classifying of the identified sites according to their characteristics (existence and size of water basins, gross head, or distance between reservoirs). Through this method, the RE100 research group from the Australian National University [29] estimated, in 2020, the potential existence of over 600,000 sites worldwide. Similarly, the European Commission estimated, in 2013, a potential of over 100,000 GWh in the territory of the member states. This study is looking for sites with an existing basin separated by up to 20 km from another basin or from a place that could accommodate an artificial one. Finally, similar studies conducted in Iran by Ghorbani et al. [32] and China by Wu et al. [34] allow us to address the interest of this method, notably for different scales and criteria.

The results obtained through the GIS method are theoretical and should be treated cautiously. However, the number of sites found is encouraging, and new topologies are being developed, letting us assume an extension of the global potential. This shows the growing interest in the development of PHSPs. In this regard, this interest should be concretized through innovations, firstly, increasing the global potential and, secondly, improving the efficiency and performance of existing PHSPs.

Recently studied with interest, the Underground PHSP (UPHSP) uses underground galleries, often from disused mines, as the lower water reservoir. Thus, while the upper reservoir is located on the surface, the penstocks, powerhouse, and other components are built underground. Although no UPHSP has yet been commissioned, technical and economic studies have resulted in encouraging perspectives. The UPHSP's primary interest is not only to increase the global potential of storage plants but also to reduce the current challenges and issues related to the flooding of natural areas and social acceptance [35,36]. According to Fan et al. [37], the advantages related to the grid (flexibility, speed, and stability) remain unchanged, while a high efficiency is maintained, which can reach 82%.

Economically, PHSPs are considered the most cost-effective storage system over their entire life cycle. Indeed, with a lifetime approaching 80 years, investments are largely repaid, and a PHSP is four to eight times cheaper than other storage technologies [26,38]. Madlener and Specht [35] claim that the investment required for a UPHSP would be only slightly higher than for a conventional plant in Germany. Also, a study conducted in Belgium indicates that it takes EUR 12 million to invest in a 100 MW UPHSP, with an estimated payback period of nine years [39]. Under these conditions, it is possible to achieve savings of 2 Mton CO_2 eq over an installation's lifetime.

Thus, the advantages appear numerous but are opposed by critical technical challenges. As Menéndez et al. [38] explained, it is essential to study the reaction of the subsoil to hydraulic surges and whether it is well prepared to accommodate the required hydraulic infrastructure. The study of water chemistry is also a challenge, as contact with the residues from former mining galleries could acidify the water and cause environmental problems in the event of leakage into nature [40].

Many authors have studied the interest of SPHSPs for marine islands that present a high potential for coupling with wind energy. Indeed, studies by the IHA [16], Katsaprakakis et al. [41], Ioakimidis and Genikomsakis [42], Katsaprakakis and Christakis [43], and Portero et al. [44] agree on the interest of islands that often cumulate high wind and solar potentials, mountainous relief, and high rainfall. A study on the islands of Curaçao [45] estimates an increase in the wind integration rate from 27 to 44% with the installation of an SPHSP, resulting in a 20% reduction in GHG emissions. Moreover, in the Canary Islands [44], energy savings are estimated at 7.68 million EUR/year, representing a payback in four years.

This article is part of a broader research initiative exploring various energy storage technologies to support the decarbonization of remote mining operations in northern Quebec. In addition to the PHSP system analyzed in this study, parallel investigations are underway on battery energy storage systems (BESS), hydrogen storage, and redox flow batteries. These complementary studies evaluate each option based on technical performance, economic viability, and environmental compatibility within off-grid Arctic contexts. However, in the context of the ongoing comparative analysis, the present paper focuses solely on the techno-economic feasibility of implementing a PHSP system at Watts Lake.

Building on this context, the present work investigates the potential for significantly reducing or even eliminating diesel dependency at the Raglan mine by integrating a wind farm with a PHSP system. Specifically, it examines how this hybrid "Diesel Thermal Power Plant–wind farm–PHSP" configuration can address the intermittency of wind energy and maintain a stable electricity supply across the mine's 25 kV-G network. The study involves the overall dimensioning of the wind–PHSP system, an assessment of its ability to meet both electricity and heating demands, and a techno-economic feasibility analysis to support future investment and implementation decisions. This study advances previous research on renewable energy integration in remote areas by addressing the unique challenges of implementing hybrid systems under extreme northern climatic conditions. Unlike traditional models that often neglect the variability of wind speeds and the harsh environmental constraints of remote locations, this research incorporates a detailed stochastic analysis of wind behavior to optimize energy generation. Additionally, integrating variable-speed hydraulic turbines within the PHSP enhances the system's adaptability to fluctuating energy demands, improving overall efficiency and reliability. By combining advanced PHSP modeling with real-world environmental constraints, this study provides a novel framework for decarbonizing off-grid industrial operations, paving the way for more sustainable and resilient renewable energy solutions in similar remote regions.

The remainder of this paper is structured as follows. Section 2 introduces the stochastic models and the role of variable-speed hydraulic turbines in enhancing the adaptability of the hybrid energy system. Section 3 outlines the methodology, including estimating electric needs, wind turbine plant design, and PHSP characteristics and sizing. Section 4 describes the modeling and simulation approach, detailing the integration of MATLAB and Excel tools to evaluate technical and economic indices. Section 5 presents the results and discussions, focusing on the proposed system's technical feasibility, economic performance, and sensitivity analysis. Section 6 validates the findings by comparing key parameters with literature and government benchmark data. Finally, Section 7 concludes the study by summarizing the key contributions and outlining recommendations for future research.

2. Stochastic Models and Variable Speed of Hydraulic Turbines

2.1. Stochastic Models

In addition to innovations that increase the potential development of PHSPs, there are trends to improve their performance. One of these uses stochastic models to optimize the operation of the storage system. The strength of this method relies on the multiplicity of possible optimizations. By predicting the output of the grid units, the weather, the energy demand, or the evolution of the electricity market, it is possible to improve the technical and economic performance of the plant. In this regard, Ding et al. [46] integrate future wind speed predictions and increase the financial benefits of generation by up to 25%.

Similarly, Bhayo et al. [47] studied rainfall to optimize the use of water volume contained in reservoirs sized to aliment a residential house. It allows the reduction in the capacity of the additional batteries initially planned to be installed by 13.12%. Although this is an uncommon application, Yahia and Pradhan [48] propose optimizing the number of pump and turbine units to limit maintenance needs. Finally, other complementary works study the prediction of wind speeds via stochastic models [49,50].

These brief examples show multiple random variables on which stochastic optimization models can be applied. For more examples, the following works present various models and methodologies that are worth studying [51–54].

This study's proposed model relies on two key components: random variables and stochastic forecasting techniques. In the context of RE–PHSP (Renewable Energy–Pumped Hydro Storage) integration, the most commonly considered sources of uncertainty in engineering applications include the following:

- Renewable energy production from various sources within the energy mix;
- Meteorological conditions (which directly affect renewable generation);
- Variations in energy demand;
- Electricity market prices in deregulated environments.

Given that this work focuses on decarbonizing the Raglan mine through the sizing and optimization of a PHSP-based hybrid energy system, the model aims to minimize the levelized cost of electricity (LCOE) while maximizing system performance. Accordingly, the outputs of the optimization process include the following:

- Economic indicators: capital and operating expenditures, energy price, payback period, and net present value (NPV);
- Technical indicators: installed capacity and power, number of wind turbines, wind penetration rate, and greenhouse gas (GHG) emission reduction.

Mathematically, the model is formulated as a stochastic optimization problem, expressed as

$$\begin{aligned} &min_{X\epsilon\mathbb{R}^N} f(X,\varepsilon) \\ &under\ stress\ g(X,\varepsilon) \leq 0 \end{aligned} \tag{1}$$

With f being the objective function, X the problem variables, ε the variable errors, and g the constrained functions of the problem.

Table 1 shows an exhaustive list of all variables, classified into four categories: fixed, sizing, performance, and feasibility.

Table 1. List and descriptions of model variables.

Variable		Characteristic	Influence
Fixed variables	Power call	Determines the needs of electricity and heat networks.	The wind farm size, the installed capacity of pumps/turbines, and the amount of water required in the reservoirs. The scenarios impose a thermal production in the balance.
	Production of wind turbines	Provides renewable power injectable into the network.	The necessary autonomy of the PHSP is caused by periods without wind and the number of wind turbines in the park to meet the power demand.
	Location	Each site has its own opportunities and limitations.	The fall, the capacity, the pressure losses, the civil engineering works, and, therefore, the CAPEX of the PHSP.
Sizing variables	Number of wind turbines	Provides the total renewable production on the network at any time.	The integration rate, and, therefore, the amount of hydraulic and thermal production required, influences the park's CAPEX and OPEX.
	Turbine power	Defines the range of electrical power that can be injected into the grid.	This parameter determines the PHSP's ability to support wind energy production and reduce reliance on thermal generation. It directly impacts both capital (CAPEX) and operating (OPEX) costs.
	Pump power	Provides the power range that can be subtracted from the network.	The power range available for pumping water. It influences the amount of wind energy lost, the rate at which the upper basin fills, and, by extension, the energy available for the turbines.
Network performance	Useful wind power production	Amount of wind energy injected into the grid directly or via turbines.	Influences the integration rate, GHG reduction, as well as OPEX of wind turbines and thermal generators.
	Turbine production	Amount of energy injected into the network via the PHSP.	Influences the integration rate, GHG reduction, as well as OPEX of wind turbines and thermal generators.
	Wind losses	Amount of surplus energy that could not be pumped.	Opens opportunities for other storage. Losses are influenced by the installed pump power, the water capacity of the reservoirs, and the number of wind turbines.
	Production of generators	Share of the energy mix remaining carbon-based.	Influences OPEX related to diesel and carbon taxes. Influences GHG emissions.
	Generator operating hours	Represents the aging rate of the generators.	Influences their lifespan and, therefore, their replacement CAPEX.

Table 1. *Cont.*

Variable		**Characteristic**	**Influence**
Feasibility	Technical feasibility	- Network's ability to meet the mine's needs through consistent operation of the production units. - Genuine benefit of the PHSP, which should significantly contribute to renewable production. - Consistency of the assumptions used, the sites studied, and the dimensions chosen.	
	Economic feasibility	- The initial investment must be feasible. - The total balance in 2037 must be positive. - Profitability must be assured before 2037.	
	GHG emissions	There is no precise indicator, but the most significant possible reduction is targeted.	

2.2. Variable-Speed Hydraulic Turbines

Recent innovations have significantly improved the efficiency and flexibility of PHSP systems. Since 1996, with the installation in Kuwabara [55] and later developments in Glodisthal in Germany (2004) and Frames 2 in Portugal (2017), several plants have adopted variable-speed pumps (VSPs) [16]. These systems connect power converters to a Constant Frequency Synchronous Generator (CFSG) or a Doubly Fed Induction Generator (DFIG), ensuring the frequency and voltage stability required for grid connection. Simultaneously, this configuration allows alternators to operate at speeds near synchronism. As Bidgoli et al. [56] and Sivakumar et al. [57] highlight, this setup enhances operational flexibility by enabling movement along the pump/turbine efficiency curve, offering a broader power range with improved efficiency.

Furthermore, studies by the IHA [16], Ghorbani et al. [32], and Joint Research Centre [33] emphasize that VSP systems outperform synchronous generators in dynamic behavior. For instance, Gao et al. [58] observed rapid power variations of up to 32 MW in generating mode and 80 MW in pumping mode within less than 0.2 s. Despite the higher initial costs due to the incorporation of power electronics [16], Feng et al. [59] demonstrated the economic viability of hybrid PV–Wind–Fuel–PHS systems using variable-speed machines. Implementing such flexible systems could reduce diesel consumption significantly, with savings ranging from 11.2% to 46.7%, depending on seasonal variations.

However, VSP systems are not without limitations. Research by the IHA [16] and Ghorbani et al. [32] points out that power converters can adversely affect power quality, and grid inertia may decrease when generators do not operate at synchronous speed. This reduction in inertia could pose challenges for grids with high renewable energy penetration.

3. Methodology

3.1. Electric Needs

3.1.1. Decarbonation Scenario

Calculating the mine's energy needs is the starting point for solving the problem since it provides the power and capacity required. First, Raglan provided the power demand for electrical devices in 2021 with a one-hour time step. Thus, the consumption amounts to 154,942 MWh with a peak power of 20 MW.

Then, it is necessary to estimate the hourly power to be decarbonized from the heat network and plan the power supply of the process by the green electricity network. It is important to note that heating the glycol water network is the only process to be electrified since ore drying requires using exhaust gases with a low CO_2 content. Referring to Figure 1, it can be seen that for the use of exhaust gases, the required electrical load must be estimated considering some EMD generators' operation.

Indeed, a continuous average production of two EMD generators operating at 2.9 MW each is sufficient to produce the required gas flow. Thus, a constant 5.8 MW of electricity can be deducted from the power demand of the 25 kV-G network. Furthermore, according to Figure 1, the HX-02 recuperator can still recover energy from combustion inside the EMD generator. Likewise, the HX-01 recuperator can also be used when the load of the EMD generator is greater than 5.8 MW, i.e., when the exhaust gas flow exceeds the needs of the drying process. It is estimated that for each megawatt of electricity the EMD generator produces, the HX-02 recuperator recovers 0.45 MW fed into the glycol network. In the same way, for every megawatt exceeding 5.8 MW, the HX-01 recuperator recovers 0.61 MW, also fed into the glycol network.

Thus, the electrical load planned to be decarbonized can be determined by summing the load of the electrical devices and the glycol network provided by Raglan. Then, it remains to subtract the constant production of 5.8 MW of electricity from the EMD generators and the 2.6 MW recovered by the HX-02 recuperator and injected into the glycol network. Figure 3 shows the details of the decarbonization process.

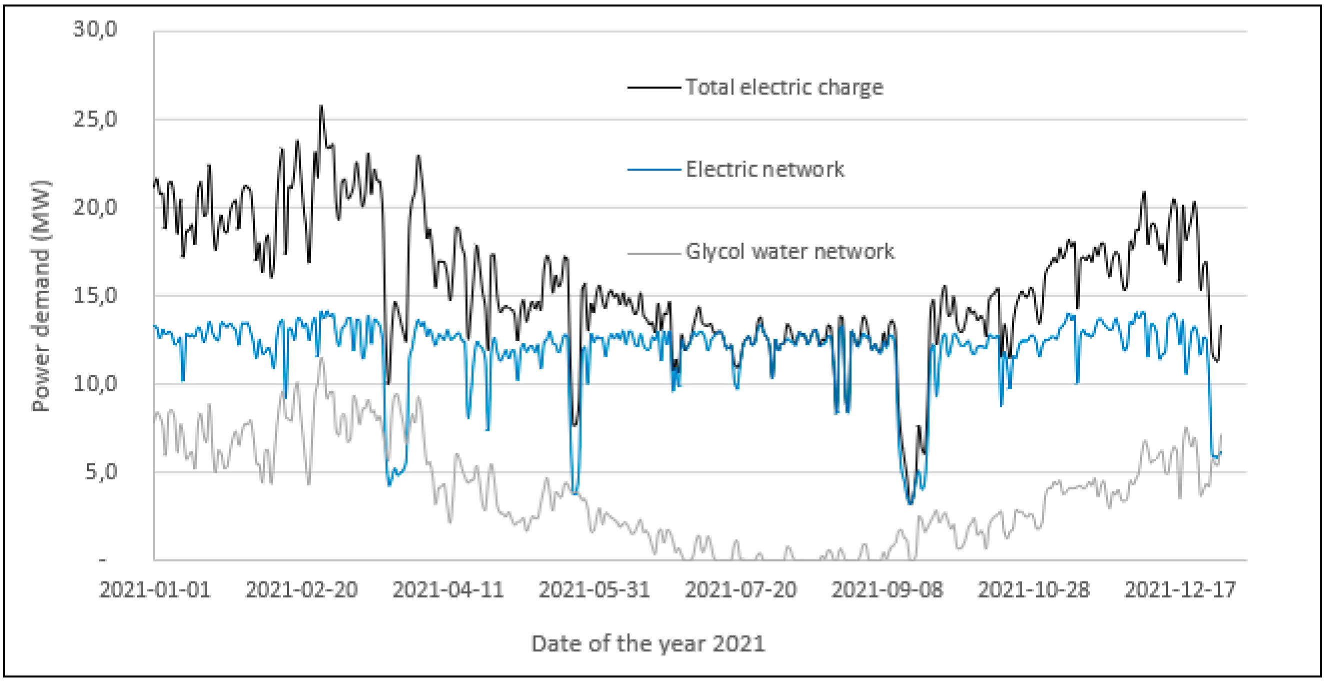

Figure 3. The power demand of the decarbonized network.

The decarbonization scenario predicts an electrical load varying between 10 and 25 MW for an annual consumption of 137,190 MWh. The share of the renewable energy target in the 25 kV-G network mix (electricity + heat) is 52.2%. For the two maintained EMD generators, producing 50,800 MWh of energy requires approximately 12.93 million liters of diesel, resulting in 35,915 tCO_2eq emissions. Thus, this scenario aims to save 25.1 million liters of diesel and 69,640 tCO_2eq emissions per year, i.e., a reduction of 66%. Moreover, it is pointed out that maintaining two EMD generators provides a certain controllable production, varying between 500 kW and 3.2 MW per unit. This is a definite advantage for the flexibility of the network, its stability, and, above all, the quality of the energy.

3.1.2. Generator Capital Expenditures (CAPEX) and Operating Expenditures (OPEX)

Based on the information provided by Raglan, it is possible to estimate the investment costs for replacing obsolete units and the lifetime and Operation and Maintenance (O&M) costs of the three generator models composing the 25 kV-G network (see Table 2).

Table 2. Generator expenditures.

Generator	Replacement	O&M	Lifetime	Spinning Reserve Units
EMD (3.6 MW)	2.6 MCAD/MW	19.2 CAD/MWh	120,000 h	2
MAN (4.5 MW)	2.6 MCAD/MW	38.5 CAD/MWh	120,000 h	1
CAT (1.8 MW)	1.5 MCAD	58.8 CAD/MWh	65,000 h	6

Finally, the costs related to diesel consumption and GHG emissions to be added to the OPEX provided in Table 2 must be evaluated. First, diesel prices are estimated using the forecasts proposed by the Energy Information Administration (EIA), available on their website [60]. Three scenarios of annual price evolution are provided from 2021 to 2050, giving bounds of 0.65 and 1.5 CAD/liter for the half-century. Moreover, regarding the estimation of pollution costs, the Canadian government and its provinces have two possible policies at their disposal. The first, known as carbon credits, is in effect in Quebec, forming a Keynesian market where the price of the right to pollute is regulated by both supply and demand and provincial control. The other policy is the carbon tax, which is more punitive, charging CAD 30 for all tons of CO_2 equivalent emitted above 50,000 tons per year. With a linear increase expected from CAD 30 to CAD 170 between 2023 and 2030, carbon taxes are more straightforward to simulate than the carbon market. Hence, this regulation was applied to the study.

Thus, knowing the details of the costs related to the operation of the generators as well as their evolution over time, all useful information is known. Then, it is easy to estimate the energy budget to be foreseen in the case of the status quo. This scenario of an unchanged energy mix is then compared to the case of the installation of the wind farm and the PHSP. Money savings are then expected from the reduction in diesel consumption, carbon taxes, and investments related to the replacement of the generators.

3.2. Wind Turbine Plant

3.2.1. Assumptions

As explained in the introduction, choosing wind energy as a renewable source is justified by the encouraging results of installing the first two wind turbines and the lack of alternative options. Indeed, given the weather conditions and the location of the mine (northern Canada, where it is extremely cold), the use of solar or hydropower does not seem relevant to cover the quantity of the 25 kV grid electrical energy demand.

Thus, the first assumption considers that the same Enercon model of 3 MW is used to construct the wind farm. Secondly, it is assumed that the historical production data for 2021 are the same for the coming years. This assumption was made following the results of a study on wind distribution. We ignore the aging and the efficiency decrease in the wind turbines over their lifetime, which is limited to 15 years (order of magnitude) due to extreme weather conditions.

These sub-hypotheses are intended to lead to a central assumption, considering that the historical hourly production of 2021 is representative, reproducible, and equal for all installed units and for their entire lifetime. This extreme assumption simplifies the solving methodology since it is sufficient to multiply the known historical production by the number of units needed to be installed to finally know the entire production of the park.

3.2.2. Wind Farm Capital and Operation Expenditures

Concerning the CAPEX and OPEX of wind turbines, Appendix A presents the methodology used to estimate variations in costs between 2023 and 2037. However, it should be noted that in 2023, the price of wind turbines is estimated at 6.23 million CAD/unit and 18.23 CAD/MWh for CAPEX and OPEX, respectively (see Figure A1).

3.3. PHSP Characteristics and Size

3.3.1. Selected Site

Among the various potential PHSP sites around Raglan mines, the Watts Lake site, located about 27 km west of Katinniq, has attracted much interest. Above the lake, the Falcon River flows through landforms before ending in this lake. The main idea is to create a dam to accumulate water in the escarpment of the riverbed. The visualization of the topography using Toporama software, 2021 version, proposed by the government of Canada [61], allowed us to visualize the two water reservoirs and estimate their volume, as seen in Figure 4.

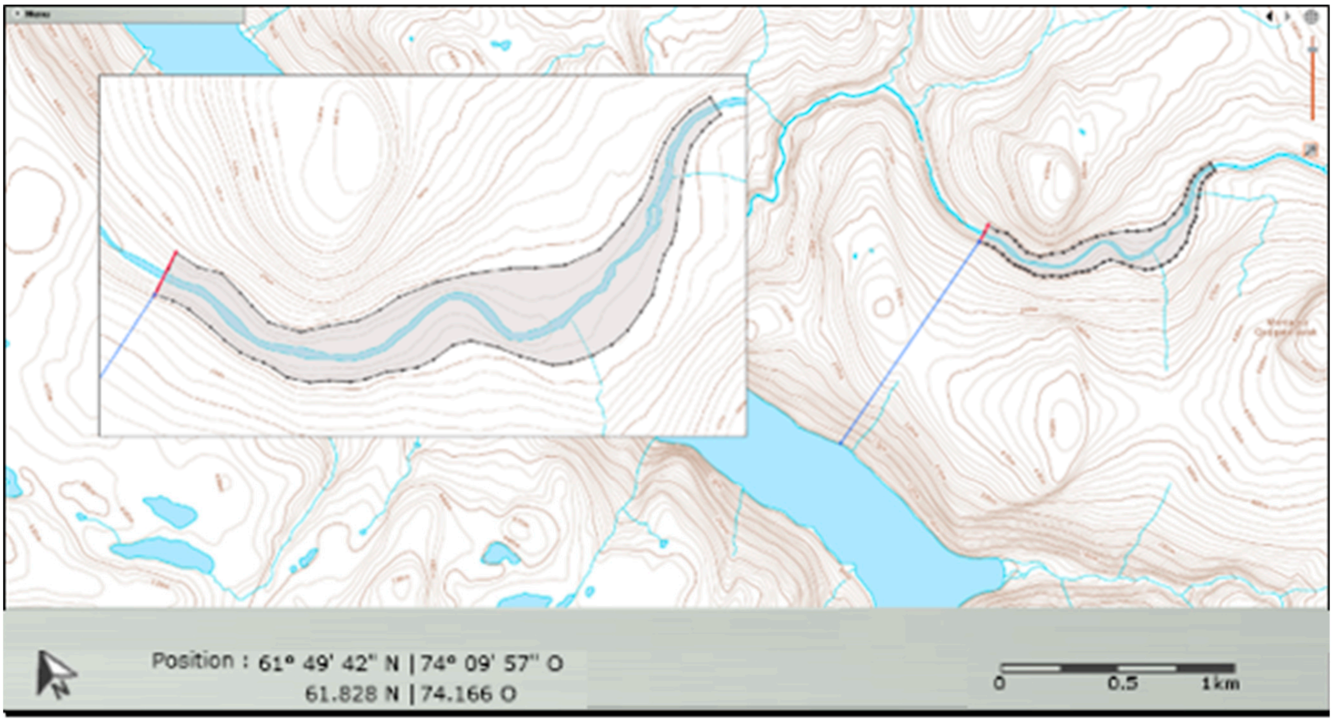

Figure 4. Location and overall span of the PHS site (map built using Toporama software, from the government of Canada: https://atlas.gc.ca/toporama/fr/index.html (accessed on 6 October 2023)).

Figure 4 shows the location of water reservoirs (in red), flooded areas (in black), and hypothetical locations of penstocks connecting to Watts Lake (in blue).

The red line shows the emplacement of the 30 m high, 200 m long dam to be constructed. Using the shape of embankment dams recommended by the US Society of Dams [62], it is possible to estimate the civil works. Thus, water retention would require approximately 230,000 cubic meters of embankment and 100,000 cubic meters of solid core. The associated costs are presented in Section 3.3.4. Next, in blue, is the location of the 2.9 km long penstocks connecting the two reservoirs with a gross head of between 160 and 190 m (depending on the water height inside the basin). Finally, the black dashed line represents the flooded area while filling the upper reservoir. The associated maximum capacity is estimated at 8.27 million cubic meters.

Although this site is relatively advantageous due to its large capacity and standard head, it suffers from two main disadvantages. The first is related to the location, as an access road and high-voltage lines must be built. According to Raglan's data, these cost CAD 700,000 and CAD 500,000/km, respectively. As a part of the road already exists, there would be 25 km to build and 40 km of high-voltage lines to install. The second challenge is related to the length of the penstocks, approaching 2.9 km. Indeed, the linear pressure losses and the excavation costs are proportional to this variable, which is singularly important compared to common sites. This constitutes the main challenge of operating the site.

Like any other part of the northern Quebec region, the area around Lake Watt is not spared from climate change. According to information from the government of Quebec [63], an increase in average temperature is expected at the end of the century, with an average temperature of 0 °C. Added to this are earlier and more significant spring floods, an increase in liquid and solid precipitation, and an increase in the number of days above freezing (in spring). Significant changes and increased fragility of ecosystems are already occurring.

3.3.2. PHSP Topology

The topology corresponds to the characteristics of hydraulic units that compose the PHSP, i.e., their power, number, type, and connection to the penstocks and electrical machines. Considering the technical and geographical characteristics of the environment, Francis turbines and centrifugal pumps were chosen. Generating and pumping modes are then distinct. Each unit operates independently of the others because they each have their own penstock and their own electrical machine. Electrical machines, motors, and generators are connected to the network by converters, allowing for variable-speed operation. Therefore, it is assumed that the efficiency of both pumps and turbines is constant, fixed at 92%, over the range of 60 to 100% of the nominal power.

The operation mode has the sets (pipelines + hydraulic machine + electrical machine) so that it is possible to reach the full range of values between the maximum installed pumping power and the maximum installed turbine power. These powers are 30 and 23 MW, respectively, determined by the optimization method in Section 5.1.1.

3.3.3. Size of Penstocks

Penstock sizes determine not only the expected excavation costs but also the flow velocity, and therefore, by extension, while considering the linear pressure losses. All these parameters depend on the pipe's length, which, for the chosen site, reaches more than 2.9 km. So, a careful selection of penstock dimensions is required, using an optimization between costs and losses to determine the appropriate diameters. The diameters thus calculated are 1.64 m and 1.51 m, respectively, for turbine and pump pipes.

Given the above, the maximum linear pressure losses are limited to 10% of the gross head, or 16 m. Depending on the hydraulic conditions, it is then easy to calculate the net head, which gives access to the flow rate once the expected power (generated or consumed power) has been calculated.

3.3.4. PHSP Capital and Operation Expenditures

Since the net head, capacity, and topology are defined, the financial parameters must be carefully considered, as the expenditures are highly dependent on the site location. Considering that the cost values proposed in the literature, given in CAD/kW and CAD/kWh, are only estimated orders of magnitude, this work is based on previous work [38,64,65] and information from the Raglan mining site, to establish an investment table below (see Table 3). The lower reservoir does not incur any costs because it is a natural reservoir. This means that there are no expenses related to excavation, embankment dam, or compacted dam costs.

Table 3. CAPEX decomposition of the PHSP.

		Quantities		Price/Unit		Source	x	Price	
Lower reservoir	Excavation	0	m^3	396	CAD/m^3	Raglan	1	0	CAD
	Solid dam	0	m^3	50	CAD/m^3		1	0	
	Embankment dam	0	m^3	20	CAD/m^3		1	0	
Upper reservoir	Excavation	0	m^3	396	CAD/m^3	Raglan [35]	1	0	CAD
	Solid dam	97,957	m^3	50	CAD/m^3		1	4,897,866	
	Embankment dam	227,607	m^3	20	CAD/m^3		1	4,552,134	
Tunnels	Excavation	22,700	m^3	396	CAD/m^3	Raglan	1	8,989,200	CAD
Road	Construction	27	km	70,000	CAD/km	Raglan	1	18,900,000	CAD
Power lines	Construction	40	km	500,000	CAD/km	Raglan	1	20,000,000	CAD
Powerhouse	Equipment Structure	26,500	kW	600	USD/kW	[38]	1	20,654,100	CAD
	Excavation	26,500	kW	97	USD/kW	[64]	2	6,678,159	CAD
DIRECT COST (DirC)								85	MCAD
Engineering and construction management Financial costs (contingency and insurance) Development costs								25% (DirC)	
INDIRECT COST								21	MCAD
TOTAL COST								106	MCAD

It can be calculated from Table 3 that the construction of roads and high-voltage lines represents 37% of the initial investment. Other expenses include the installation of the powerhouse, penstocks, and water reservoir. By multiplying factors on prices given in the literature, it is possible to consider the location of the Raglan mine in the expected cost increase. Thus, the investment is estimated to be around 4000 CAD/kW, corresponding to a 50% increase compared to the data found in the literature [26].

Appendix B presents the methodology used to estimate O&M costs. Unlike the price of diesel, carbon taxes, and wind turbine O&M, the value for PHSP is fixed and estimated at 72.5 CAD/kW-year.

4. Modeling and Simulations

4.1. Project Variables

4.1.1. Input Data

All parameters determined in the precedent sections are data used for simulations. This includes the hourly power demand, the wind generation for 2021, and all natural and calculated characteristics of the PHSP. In addition to these fixed variables, some are considered modifiable for optimization purposes, including the number of wind turbines and the power installed for both turbines and pumps.

4.1.2. Output Data

The output data are also divided into two categories, starting with technical indices:

- The network's ability to meet the electricity needs of the mine;
- The renewable integration rate and the PHSP's ability to significatively increase this rate.

The coherence of the chosen dimensions is assessed by the evolution of the water volume inside the upper basin and by the amount of wind energy thrown out (see Section 5.1.1).

Secondly, financial indices were determined to evaluate the economic feasibility of the project:

- The net present value (NPV) is calculated using both a discount and an inflation rate. Following the report [66], their respective values are implemented at 8 and 2%:
  - The payback period,
  - The initial investment required.

All those indices were obtained thanks to the MATLAB algorithm and the Excel program presented in the next section. Then, the results for the above-mentioned outputs are summarized in Section 5.

4.2. Algorithm and Programming

4.2.1. MATLAB Program

To assess the validity of the techno-economic indices, it is necessary to implement grid operations for wind and PHSP installation. The MATLAB program, whose role is to simulate the grid, comprises two main parts. The first defines the characteristics of production units (diesel, wind, and hydro), while the second is a loop that compares power demand and wind production. These latter are evaluated at the hourly time step. Whether it results in a lack or excess production, the program then compensates with a response from the PHSP and diesel generators. This operation is repeated 8760 times, representing an hourly simulation for an entire year. Moreover, the evolution of the volume available in the PHSP is also monitored to validate, in part, the consistency of the sizing. For more details, Appendix C provides the flowchart of the main loop and a more precise description.

The MATLAB program provides the annual production of wind turbines, hydraulic turbines, pumps, and various generator models. The renewable integration rate, the wind energy losses, the energy deficit, and the operating hours of each diesel generator model are also known. These data and the technical and financial parameters presented above allow for assessing the project's feasibility.

4.2.2. Technical and Economic Analysis

The techno-economic analysis was conducted via an Excel program that uses all the information generated on MATLAB. By associating this information with the known economic parameters, it is possible to calculate the price of thermal, wind, and hydraulic energy for the simulated year. This operation can then be repeated, considering the evolution of specific parameters (the price of diesel, carbon taxes, wind power OPEX, etc.) to determine the evolution of the price of energy between 2023 and 2037. Those dates correspond to the theoretical beginning of the project and the end of the mining exploitation license. By adding, for the year 2023, the wind and hydro CAPEX, as well as the generator replacement CAPEX, if necessary, it is possible to know the total and annual price of energy on the 25 kV-G network for the next fifteen years. In parallel, the same work is done for the status quo scenario, which gives access to the yearly savings, thanks to renewable production. These last collected data allow us to follow the evolution of the recovery of the initial investment.

4.2.3. Aspects Related to Energy Sizing

The energy production capacity of the PHSP system was sized based on three main factors: the energy demand of the Raglan mine, the projected output of the planned wind farm, and peak demand conditions. The PHSP sizing process takes into account the following key parameters:

- Head height: This is site-specific and represents the naturally available hydraulic head, directly influencing the potential power output.
- Storage capacity: Defined by the volume of the upper and lower reservoirs, this determines the energy autonomy of the PHSP system—i.e., the duration for which it can operate at maximum output without recharge. This factor is essential in supporting a high share of variable renewable energy on the local grid.
- Flow rate: This is the primary controllable variable and plays a key role in system performance. The maximum flow rate influences the dimensioning of penstocks and turbines and pressure losses within the system.

Using these parameters, the hybrid energy system was optimized through a techno-economic approach aimed at minimizing the levelized cost of electricity (LCOE), maximizing the net present value (NPV), and achieving the shortest possible return on investment (ROI). While economic and technical indicators are crucial in project evaluation, this study's primary objective remains reducing greenhouse gas (GHG) emissions. As such, GHG reduction is the central evaluation criterion guiding the overall system design.

Technological advances in wind turbine engineering have further contributed to system performance by improving energy yield and durability. These improvements are largely due to advanced materials that reduce turbine weight and increase efficiency, such as lightweight composites (e.g., carbon fiber or high-strength polymer fibers). These innovations also enable wind turbines to operate more effectively at low wind speeds, thereby reducing variability and improving overall system reliability [67].

5. Results and Discussions

5.1. Dimensions and Performances

5.1.1. Technical Feasibility

Table 4 summarizes the main technical parameters obtained following the simulations.

Table 4. Technical performances of the grid.

Variables	Results	Units
Number of wind turbine	17	Dimensionless
Hydraulic turbine power	23	MW
Hydraulic pump power	30	MW
Wind energy used	126,000	MWh/year
Wind energy lost	9700	MWh/year
Hydraulic turbine generation	40,200	MWh/year
Liters of diesel consumed	14.6	ML/year
Total GHG emissions	40,500	tCO_2eq/year
Need to install a new generator	None	Dimensionless
Renewable energy rate compared to the grid	48.1	%
Renewable energy rate compared to the objective	91.8	%
Energy deficit	0	MWh

A distinction is then made between sizing variables and grid performance parameters. Referring to the technical feasibility indices, it can be concluded that:

- The energy deficit is zero, which means that the production units meet all the network needs;

- The production of the turbines represents 25% of the energy mix targeted by decarbonization, which proves the importance of the PHSP. Moreover, the "renewable energy rate compared to the objective", which refers to this share of the energy mix, reveals satisfactory results as 91.8% of the target is reached.

The last point to check is the consistency of the chosen dimensions for the wind and hydro installations. This is based both on the energy losses of the wind turbines and on the evolution of the water volume in the upper reservoir. Figure 5 illustrates all of the above.

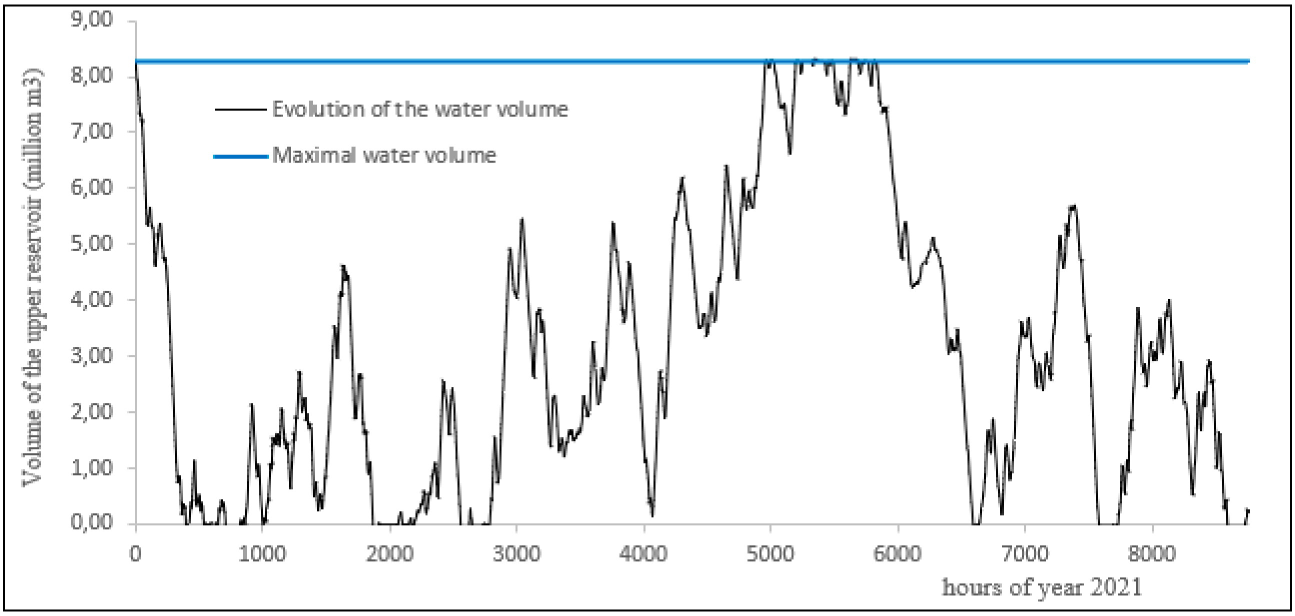

Figure 5. Evolution of the water volume into the upper reservoir.

The variation in water volume over the year gives an overall idea of the wind and hydraulic sizing quality. Indeed, if the events of water shortage are the most frequent, it can be expected that the pump power is under-dimensioned (limiting the energy absorption) or that the wind farm is under-dimensioned (requiring the use of turbines too frequently). On the other hand, if excess water is too frequent, it means that the pumping capacity or the wind farm is oversized. The second case is problematic since the initial investment would be too high. Thus, a relatively optimized system involves an appropriate balance between its shortage and excess episodes.

Figure 6 represents the average daily power outputs calculated from the hourly power outputs recorded in 2021 on the two Enercon E82 E4 turbines installed.

5.1.2. Economic Feasibility

Table 5 shows the OPEX and CAPEX of the generation units throughout the project. Notably, a distinction is made between the CAPEX of the wind turbines, planned to be installed in 2023, and the investment required to replace the two initial units (expected in 2032). In addition, using the cost and output decomposition given in Table 5, the wind, hydro, and thermal energies' levelized costs of energy (LCOEs) can be estimated at 69, 206, and 202 CAD/MWh, respectively. In comparison, for the status quo, the overall LCOE is 256 CAD/MWh, which explains the profitability of the installations. Indeed, Table 6 provides the economic feasibility indices presented in Section 4.1.2.

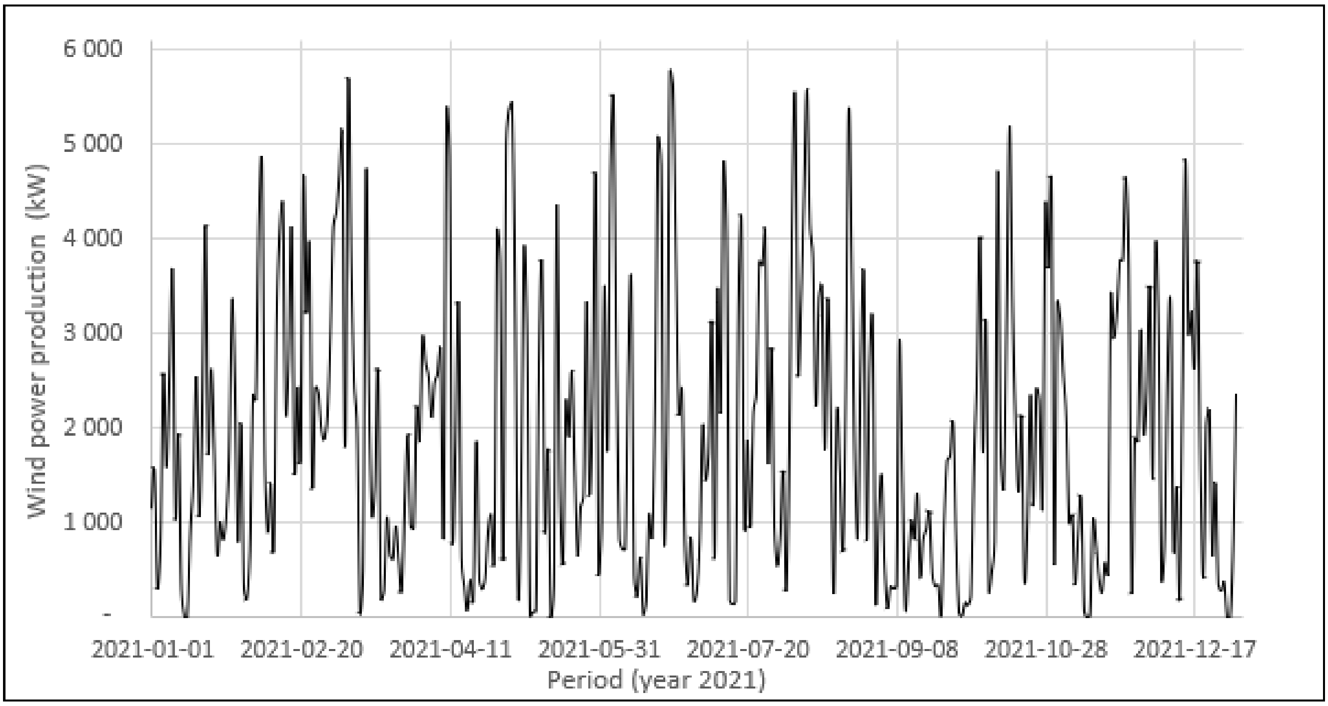

Figure 6. Daily power produced by the two Raglan wind turbines in 2021.

Table 5. Total CAPEX and OPEX over the life of the project.

Sources	Price (MCAD)
Diesel	191
Carbon taxes	0
Maintenance	17
Replacement	0
Total generator cost	208
Wind OPEX	37.6
Wind CAPEX 2023	93.5
Wind CAPEX 2032	9.4
Total wind cost	140.5
PHSP OPEX	28.8
PHSP CAPEX	135
Total PHSP cost	163.8
Total cost	512.3

Table 6. Financial indices.

Index	Price	Units
Total discounted cost	346	MCAD
Net present value (NPV)	5.6	MCAD
Total cost without discount	512.3	MCAD
Final balance without discount	122	MCAD
Payback	2034	Dimensionless
Average OPEX without discount (15 years)	18.3	MCAD/year
CAPEX in 2023 without discount	228.5	MCAD

Through these results, the real influence of the discounting of the monetary value can be seen since, once it is considered, the project balance is barely positive. On the other hand, without considering it, profitability is assured in 2034, with a final saving of 122 million CAD for an initial investment of 200 million CAD.

Thus, it can be concluded that with the chosen assumptions, the proposed study framework and the simulation method indicate an encouraging technical and economic feasibility. However, to conclude more confidently, a few additional studies need to be carried out, mainly to validate certain conditions or clarify constraints that have been overlooked.

5.2. Discussion and Complementary Studies

5.2.1. Discussion on the Main Hypothesis

In this section, we analyze the hypotheses that seem to be the most questionable. The first debatable assumption is the one about the reproducibility of the 2021 wind production, which is considered identical for the next fifteen years and all the installed units. This production is bound to change, either due to natural changes in wind speeds or the aging of the turbines. Similarly, the second questionable assumption is that the grid energy demand shall remain unchanged until the end of the mine exploitation. In fact, it is supposed to increase from 2023 and then decrease in the last years of operation, but it has been chosen to keep it constant to simplify the study. Finally, to facilitate the resolution, the price of pollution was calculated using the carbon tax policy and not from the carbon market specific to Quebec. Thus, the results obtained, which otherwise greatly support the project's economic feasibility, may differ somewhat from reality.

5.2.2. Complementary Studies

To go further in the realization of this project and to complete the pre-feasibility assessment stage, it could be relevant to study the following three main points. First, it is necessary to prove a genuine interest in Watts Lake by studying, among other things, the access to the site, the expected environmental impact, and the jurisdiction related to creating a structure on Inuit territories. Indeed, no preliminary study has been conducted to ensure the site could be exploited. The second would be related to the estimation of the wind generation, which could be assessed with greater precision. For this, it would be necessary to determine the optimal location for the wind farm installation to deduce the associated production. In addition, considering the use of more powerful turbines could lead to a reduction in the size of the wind farm and possibly a reduction in investment costs. Finally, it seems necessary to investigate the power quality, the frequency and voltage stability, and the power driving options to control precisely all units' production. Indeed, these last criteria are undeniably required to respect all network norms.

6. Results Validation

Although finding works in a similar configuration to the present one in the literature is challenging, a comparative analysis is carried out to validate the model's key parameters. The costs associated with the creation and operation of the PHSP, GHG emissions, and the overall performance of the PHSP were retained as key parameters for comparison. Regarding the cost of the PHSP, the predictions of this model are very close to those mentioned in the work of Madler and Specht [35] (see Table 7 below). As for GHG emissions, the value of 40,500 t CO_2 eq/year, found in this model, is well within the lower limit (i.e., less than 50,000 t CO_2 eq/year) from which carbon taxes are imposed by the government of Canada [68], which shows that the decarbonization objectives of the Raglan Mine site have been achieved (see Table 7 below). Finally, the yield of PHSP equipment in this model is consistent with the yields mentioned by the IHA [26].

Table 7. Comparison with different results in the literature and errors in the simulation.

Cost of PHSP [CAD/kW installed]		
Madler and Specht [35]	**Present model**	**Difference**
2925–4680	3100–4000	14.53%
GHG emissions [t CO_2 eq/an]		
Government of Canada [68]	**Present model**	**Margin**
50,000	40,500	19%
Yield of PHSP [-]		
IHA [26]	**Present model**	**Error**
0.86	0.85	1.16%

The use of bold and background color is to highlight the labels and what is being compared. It is also to separate two different comparisons.

Since the proposed hybrid wind–PHSP system has not yet been implemented at the Raglan mine, real-world operational data are currently unavailable for direct validation. As an alternative, we adopted a benchmarking approach, comparing our model outputs with results from similar studies found in the literature. These reference studies were selected based on comparable characteristics, such as using pumped hydro storage in remote or isolated contexts, integration with variable renewable energy sources, and shared decarbonization objectives. The validation focused on three key variables, system cost, energy performance, and GHG emissions reduction, and revealed strong consistency, particularly regarding PHSP efficiency and economic metrics. This comparative analysis provides a reliable basis for assessing the model's credibility without site-specific performance data.

Based on the above information, predictions, and comparisons, the results of this model can be considered reliable and valid.

7. Conclusions

To meet GHG emission limitation requirements, the Raglan mining company has prioritized the decarbonization of its operations, focusing specifically on its electricity production system. Given that Raglan Mine wishes to increase the integration rate of renewable energies in its energy mix, this work focused on the Raglan Mine site's local electricity and heat network.

The evaluation and validation of the results were done using technical indices, which question the electrical production units' capacity to meet the mine's energy needs.

Regarding the financial aspects, annual energy prices from 2023 to 2037, for both the renewable hybrid system and the case of the status quo, were calculated. Three financial indices were deduced: the final balance, the return on investment period, and the initial investment to be expected in 2023.

The results obtained also showed that the site chosen for the installation of the PHSP can meet the objectives of reducing current diesel consumption by 60%. The three technical and financial criteria mentioned above were also validated since the return on investment period is 11 years.

Furthermore, without considering discounting and inflation rates, the final balance is positive and amounts to more than 120 million CAD in 2037, compared to the status quo, for an initial investment of 200 million CAD. The investment costs of the wind turbines and the PHSP are estimated at CAD 1830/kW and CAD 4000/kW, respectively, while the OPEX are estimated at CAD 18.4/MWh and CAD 72.5/kW-year. The results show investment costs of CAD 2080/kW and CAD 3720 CAD/kW, respectively, for the wind farm and the PHSP. As for the operating costs, the values of 17.3 CAD/MWh and 72.5 CAD/kW-year were found for the wind farm and the PHSP.

While this study successfully demonstrates the techno-economic feasibility of integrating a wind farm with a PHSP system to decarbonize the Raglan mine, it is essential to note that detailed power quality aspects, such as voltage fluctuations, frequency regulation, and grid inertia management, are not covered within the current analysis. Our modeling approach focuses on energy balance and cost assessments and does not include dynamic simulations of grid stability. These power quality considerations are critical for ensuring reliable operation under high renewable penetration and extreme weather conditions and will be addressed in a subsequent study using specialized power systems analysis tools.

The detailed feasibility study of implementing a PHSP at Watts Lake is undoubtedly the most important next step. It is a question of evaluating in much more detail the costs, the access to the site, and the possibility of building infrastructures, regarding both the topography constraints and, especially, the influence of frost (because of the location in the northern region of Canada, with extremely negative temperatures) on the behavior of the pumping plant.

Future work will also focus on conducting a detailed sensitivity and probabilistic analysis to evaluate the impacts of uncertainties related to wind variability, water availability, energy demand, and long-term climate conditions on the system's performance and reliability.

Thus, there remains a wide range of studies that future work could tackle to finalize the present project.

Author Contributions: Conceptualization, A.T. and D.R.R.; methodology, A.T., D.R.R., B.-J.R.M.B. and A.I.; software, A.T.; validation, D.R.R. and B.-J.R.M.B.; formal analysis, A.T., D.R.R., B.-J.R.M.B. and A.I.; investigation, A.T. and D.R.R.; resources, D.R.R.; data curation, A.T.; writing—original draft preparation, A.T., D.R.R. and B.-J.R.M.B.; writing—review and editing, D.R.R. and A.I.; visualization, A.T. and B.-J.R.M.B.; supervision, D.R.R.; project administration, D.R.R.; funding acquisition, D.R.R. All authors have read and agreed to the published version of the manuscript.

Funding: The authors thank Glencore and Hatch industrial partners for their support during this project. They also acknowledge the FRQ-NT for its financial support via grant 322720 and the Michel Trottier private donation to the t3e research group.

Data Availability Statement: The original contributions presented in the study are included in the article, further inquiries can be directed to the corresponding author.

Acknowledgments: The authors acknowledge the data and information from the industrial partners Glencore and Hatch.

Conflicts of Interest: The authors declare no conflicts of interest.

Declaration of Generative AI and AI-Assisted Technologies in the Writing Process: The authors did not use generative AI technologies while preparing this work. The authors used AI-assisted technologies, Grammarly (www.grammarly.com) and Antidote (www.antidote.info), to improve formulation and eliminate grammatical errors. After using this tool/service, the authors reviewed and edited the content as needed and take full responsibility for the publication's content.

Appendix A

The present paper and the Appendices A–D describe all the data and processes.

Figure A1 represents the expected evolution of the CAPEX and OPEX of wind turbines.

These results were obtained by referring mainly to the work of Sens et al. [69] and Wiser et al. [70], who provide cost projections based on actual prices from 2012 for CAPEX and 2018 for OPEX. Then, these costs were re-evaluated by considering the decomposition of investment and maintenance costs, respectively proposed by Stehly et al. [71], from the National Renewable Energy Laboratory (NREL) and by Wiser et al. [70]. Thus, the visualization of the different expenses allows us to judge those dependent on the insular location of the mine, such as the creation of the foundations. These parameters were then doubled to consider the location of Raglan, which provides a new cost projection. Moreover, as the results of the above works are given in euros and US dollars, the currencies are converted back to Canadian dollars using the historical monthly conversion values provided by the Canadian government website between 2017 and 2022 [72]. The rates were then estimated at 1.299 CAD/USD and 1.498 CAD/EUR.

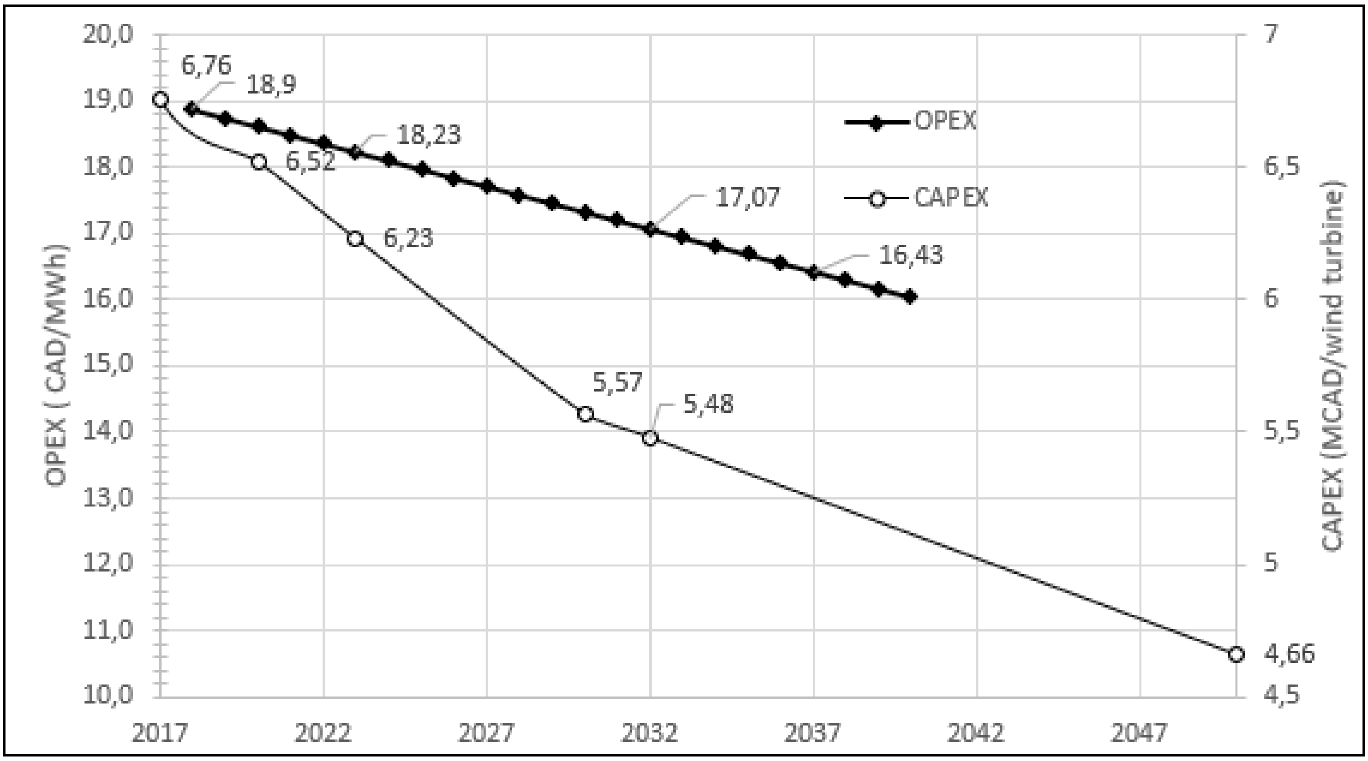

Figure A1. Wind turbines CAPEX and OPEX projections.

Appendix B

Similarly to wind turbines, the O&M costs of the PHSP were determined using an expenditure breakdown provided by Oladosu and Sashav (2022) [65]. Thus, all expenses influenced by the location of the mine were doubled, e.g., maintenance of the dam or the power plant. Then, the OPEX, initially estimated at 39 USD/kW-year, was recalculated to 55.8 USD/kW-yr, i.e., a fixed cost of 72.5 CAD/kW-year. In contrast to the costs of wind turbines, it is assumed that no evolution is expected in the coming years due to the maturity of hydro technologies.

Appendix C

This last appendix presents the flowchart used in the MATLAB program to simulate the network operation and all the production units. Figure A2 below represents the main loop.

First, the wind generation and the power demand of the grid are compared to determine the expected operating mode of the PHSP. Thus, in case of an energy lack, the pumps and turbines are activated to obtain, at best, the missing power. The opposite is also true for pumping in cases of excess production. So, the terms "turbines" and "pumps" only represent the global operation mode of the PHSP since all units can work simultaneously to obtain a final expected production or consumption. After determining the power to be deployed, it is possible to determine the net flow. Indeed, it is possible to calculate the gross flow rate and the associated head losses from the gross head and the expected power to obtain the net flow rate. It is through this variable that, at the end of the loop, it is possible to calculate the accurate volume gained or lost in the upper reservoir.

Then, once all parameters of the PHSP are determined, the operation of the generators remains to be established. In the case of excess energy, the auxiliary generators are not required. There is, therefore, no deterioration of the machines and no energy deficit. On the other hand, the power surplus may be even more significant than the pumping capacity, in which case the energy dissipation is accounted for observation purposes.

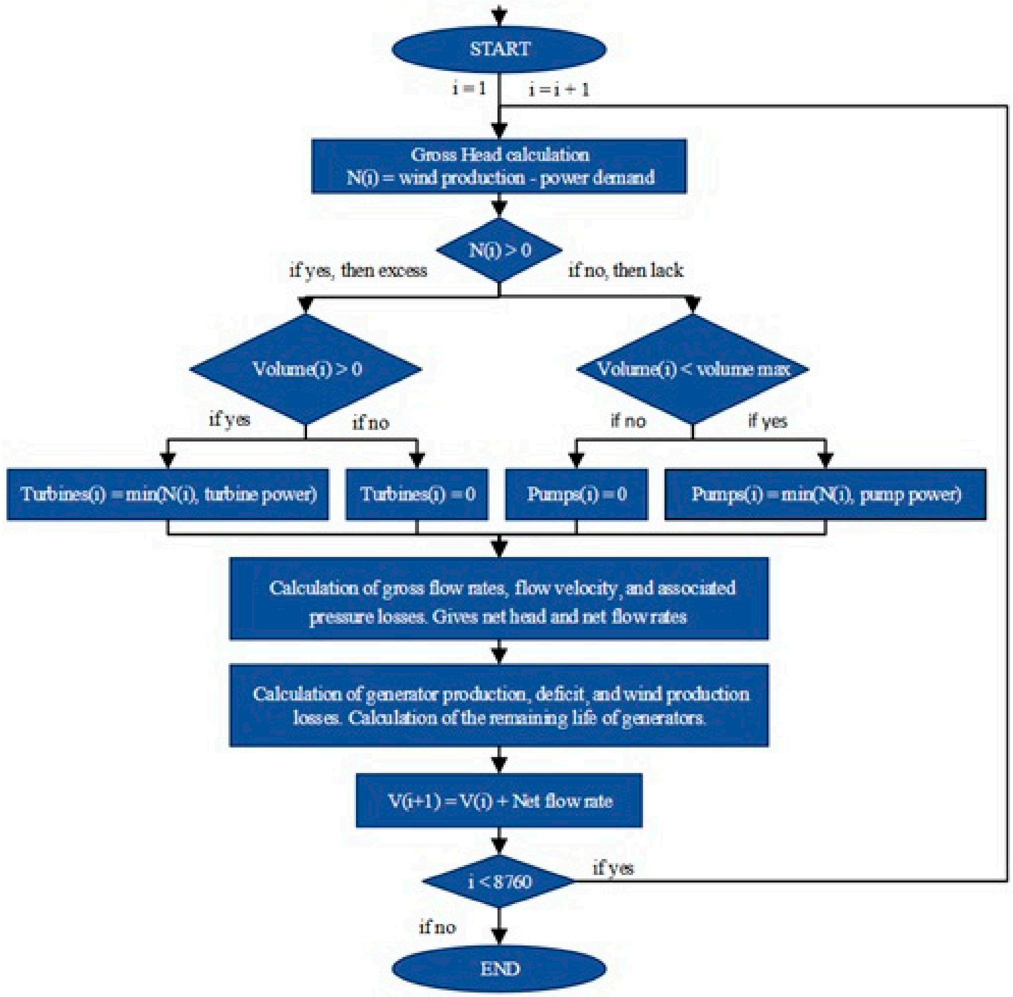

Figure A2. Flowchart of the main loop.

However, in the case of an energy shortage that exceeds the turbine capacity, there is a risk of an energy deficit. The energy deficit can be avoided by activating the EMD, MAN, and CAT generators in this order. On the other hand, the number of generators operated is then counted to know each unit's total hours of operation at the end of the year. The remaining lifetime can then be estimated, and the possible replacement needs can be estimated. The generator orders follow the process shown in Figure A3.

This last figure shows the effects of cogeneration in saving the electricity required. Indeed, when the wind turbines and the PHSP cannot fully meet the needs, the EMD generators are switched on. However, for each megawatt produced, the HX-01 and HX-02 heat exchangers recover 1.06 megawatts sent to the glycol network, which are therefore deducted from the overall electricity demand. Thus, at best, the EMD generators can supply $2.06 \times 2 \times 3.2$ MW of power. Beyond that, it is the MAN and the CAT generators that take over. The number of generators used is then calculated, which gives the total operating hours at the end of the year.

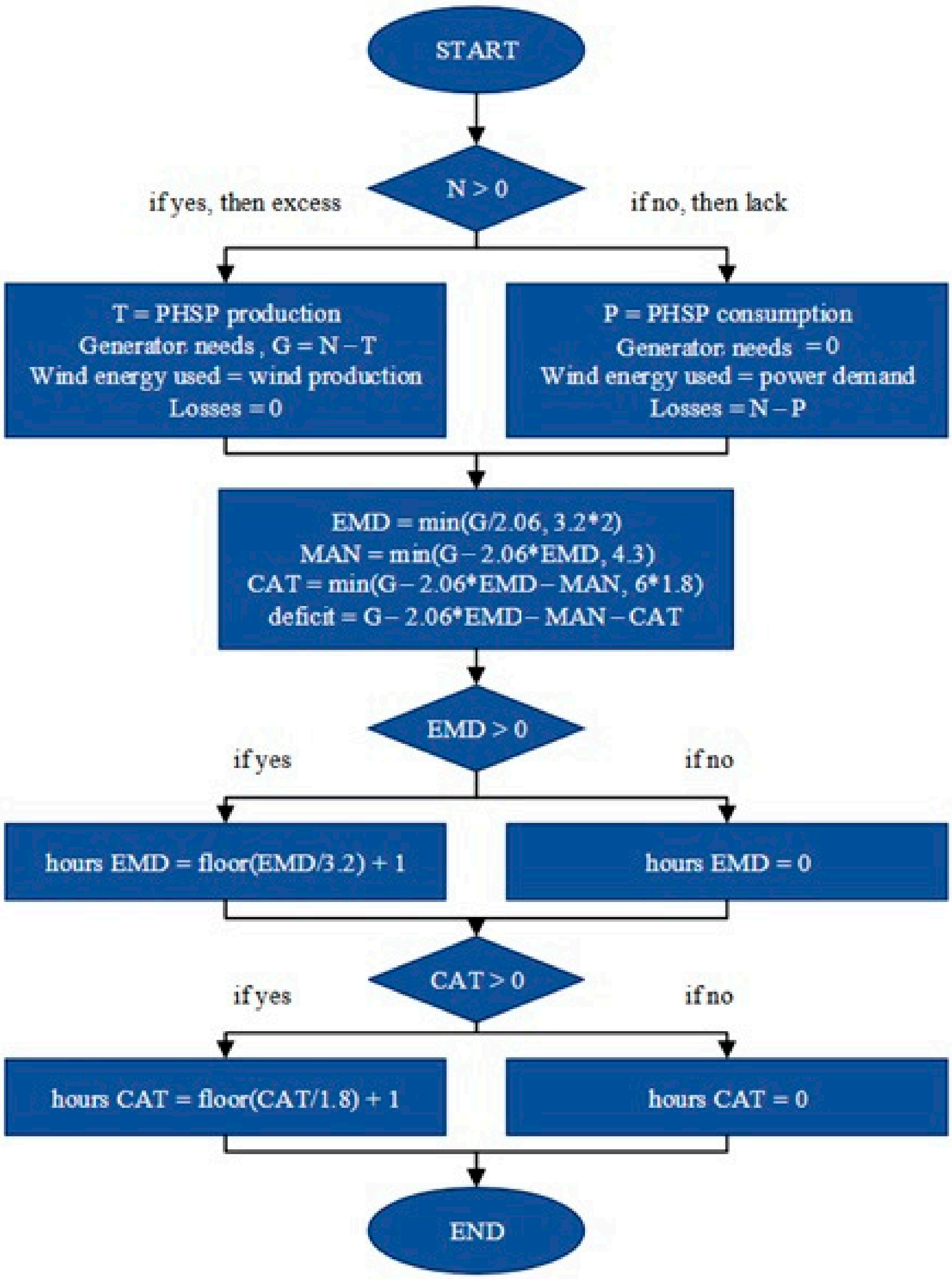

Figure A3. Flowchart of the generators' commands.

Appendix D

Table A1 gives a summary of the main equations used in this model.

Table A1. Main equations used in this model.

Equation	Variable	Observation	Meaning of Terms
$\Delta H_{reg} = \lambda \frac{U^2 L}{2gD}$	Linear pressure losses	Definition of the nature of the flow: $Re = U * D/\nu$ Kinematic viscosity of water, $\nu = 1.68 \times 10^{-6}$ m^2/s If Re < 2000, the flow is laminar and λ = 64/Re according to the Hagen–Poiseuille law. On the other hand, if Re > 3000, then the regime is turbulent, and the coefficient can be determined by several laws or graphically via the Moody diagram.	$\begin{cases} L: \ length\ of\ hydraulic\ pipes\ [\mathrm{m}] \\ D: \ diameter\ of\ hydraulic\ pipes\ [\mathrm{m}] \\ U: \ flow\ velocity\ [m/s] \\ \lambda: \ friction\ coefficient \end{cases}$ Re: Reynolds number
$Q = U * \frac{\pi D^2}{4}$	Hydraulic flow		$U: flow\ velocity\ [\mathrm{m/s}]$
$Actual\ Value = Value * \frac{(1+i)^{N-1}}{(1+t)^N}$	Net present value (NPV)	Each investor is free to choose their own inflation and discount rates to judge the economic feasibility of their projects.	$\begin{cases} N: \ the\ number\ of\ years\ separating\ the\ expenditure \\ from\ the\ expenditure\ from\ the\ discount\ date \\ i: the\ inflation\ rate \\ t: the\ discount\ rate \end{cases}$
$H_{net} = H_{raw} \pm \Delta H_{reg} \pm \Delta H_{sing} = \begin{cases} H_{raw} - \lambda \frac{U^2 L}{2gD} - \zeta \frac{U^2}{2g} \ \ in\ turbine \\ H_{raw} + \lambda \frac{U^2 L}{2gD} + \zeta \frac{U^2}{2g}\ in\ pumping \end{cases}$	Gross drop	The gross drop corresponds to a real difference in altitude between the inlet and the outlet of the hydraulic network.	$\begin{cases} H_{raw} = Gross\ head\ [\mathrm{m}] \\ L: length\ of\ hydraulic\ pipes\ [\mathrm{m}] \\ D: \ diameter\ of\ hydraulic\ pipes\ [\mathrm{m}] \\ U: flow\ velocity\ [m/s] \\ \lambda: linear\ head\ loss\ coefficient \\ \zeta: singular\ head\ loss\ coefficient \end{cases}$
$\begin{cases} P_{injected\ into\ the\ network} = \eta_{generator} * \ \eta_{turbine} * \rho \ * g * H_{net} * Q \\ P_{subtracted\ from\ the\ network} = \frac{\rho * g * H_{net} * Q}{\eta_{motor} * \ \eta_{pump}} \end{cases}$	Hydraulic power	From these equations, an analogy with electrical quantities can be observed.	$\begin{cases} \eta_x = efficiency\ of\ hydroelectric\ machines \\ \rho: the\ density\ of\ water\ [\mathrm{kg/m^3}] \\ g: the\ constant\ of\ gravity\ [9,81\ \mathrm{m/s^2}] \\ H_{net}: the\ net\ head\ [\mathrm{m}] \\ Q: the\ flow\ rate\ [\mathrm{m^3/s}] \end{cases}$
$min_{X \epsilon \mathbb{R}^N} f(X, \varepsilon)$ $under\ stress\ g(X, \varepsilon) \leq 0$	Stochastic optimization problems	This work uses stochastic forecasting models, which are mathematical models that consider the probable error inherent in the chosen parameters.	With f being the objective function, X the problem variables, ε the variable errors, and g the constrained functions of the problem.

References

1. United Nations Framework Convention on Climate Change. *Report of the Conference of the Parties on Its Twenty-First Session, Held in Paris from 30 November to 11 December 2015—Part One: Proceedings*; United Nations Framework Convention on Climate Change: Paris, France, 2016; p. 42.
2. Government of Canada. *Greenhouse Gas Emissions Canadian Environmental Sustainability Indicators*; Environment and Climate Change Canada: Gatineau, QC, Canada, 2025.
3. Jahangiri, Z.; Hendriks, R.; McPherson, M. A Machine Learning Approach to Analysis of Canadian Provincial Power System Decarbonization. *Energy Rep.* **2024**, *11*, 4849–4861. [CrossRef]
4. Government of Canada. Canada's Official Greenhouse Gas Inventory. Annex 13—Electricity in Canada. Available online: https://open.canada.ca/data/en/dataset/779c7bcf-4982-47eb-af1b-a33618a05e5b (accessed on 9 January 2025).
5. Government of Canada. Canadian Net-Zero Emissions Accountability Act. Available online: https://www.canada.ca/en/services/environment/weather/climatechange/climate-plan/net-zero-emissions-2050/canadian-net-zero-emissions-accountability-act.html (accessed on 9 January 2025).
6. Saffari, M.; McPherson, M. Assessment of Canada's Electricity System Potential for Variable Renewable Energy Integration. *Energy* **2022**, *250*, 123757. [CrossRef]
7. Du, Y.; Shen, X.; Kammen, D.M.; Hong, C.; Nie, J.; Zheng, B.; Yao, S. A Generation and Transmission Expansion Planning Model for the Electricity Market with Decarbonization Policies. *Adv. Appl. Energy* **2024**, *13*, 100162. [CrossRef]
8. Balaban, G.; Dumbrava, V.; Lazaroiu, A.C.; Kalogirou, S. Analysis of Urban Network Operation in Presence of Renewable Sources for Decarbonization of Energy System. *Renew. Energy* **2024**, *230*, 120870. [CrossRef]
9. Dongsheng, C.; Ndifor, E.Z.; Temidayo Olayinka, A.-O.; Ukwuoma, C.C.; Shefik, A.; Hu, Y.; Bamisile, O.; Dagbasi, M.; Uzun Ozsahin, D.; Adun, H. An EnergyPlan Analysis of Electricity Decarbonization in the CEMAC Region. *Energy Strategy Rev.* **2024**, *56*, 101548. [CrossRef]
10. Obiora, S.C.; Bamisile, O.; Hu, Y.; Ozsahin, D.U.; Adun, H. Assessing the Decarbonization of Electricity Generation in Major Emitting Countries by 2030 and 2050: Transition to a High Share Renewable Energy Mix. *Heliyon* **2024**, *10*, e28770. [CrossRef]
11. Roshan Kumar, T.; Beiron, J.; Marthala, V.R.R.; Pettersson, L.; Harvey, S.; Thunman, H. Combining Exergy-Pinch and Techno-Economic Analyses for Identifying Feasible Decarbonization Opportunities in Carbon-Intensive Process Industry: Case Study of a Propylene Production Technology. *Energy Convers. Manag. X* **2025**, *25*, 100853. [CrossRef]
12. Paraschiv, L.S.; Paraschiv, S. Contribution of Renewable Energy (Hydro, Wind, Solar and Biomass) to Decarbonization and Transformation of the Electricity Generation Sector for Sustainable Development. *Energy Rep.* **2023**, *9*, 535–544. [CrossRef]
13. Wang, X.; Bamisile, O.; Chen, S.; Xu, X.; Luo, S.; Huang, Q.; Hu, W. Decarbonization of China's Electricity Systems with Hydropower Penetration and Pumped-Hydro Storage: Comparing the Policies with a Techno-Economic Analysis. *Renew. Energy* **2022**, *196*, 65–83. [CrossRef]
14. Lee, H.; McJeon, H.; Yu, S.; Liu, Y.; Kim, H.; Eom, J. Decarbonization Pathways for Korea's Industrial Sector towards Its 2050 Carbon Neutrality Goal. *J. Clean. Prod.* **2024**, *476*, 143749. [CrossRef]
15. Onodera, H.; Delage, R.; Nakata, T. The Role of Regional Renewable Energy Integration in Electricity Decarbonization—A Case Study of Japan. *Appl. Energy* **2024**, *363*, 123118. [CrossRef]
16. IHA. *Innovation Pumped Storage Hydropower Configurations and Uses*; IHA: London, UK, 2021.
17. Zhao, K.; Wang, J.; Qiu, L. Approval and Progress Analysis of Pumped Storage Power Stations in Central China during the 14th Five-Year Plan Period. *J. Energy Storage* **2024**, *102*, 114104. [CrossRef]
18. Silva, C.S.; Couceiro, D.; Castro, R.M.G. The Role of Pumped Hydro Storage in the Portuguese National Plan for Energy and Climate for 2030: A Hybrid Approach Using Energy PLAN and Machine Learning. *J. Energy Storage* **2024**, *103*, 114194. [CrossRef]
19. Jing, Z.; Wang, Y.; Chang, J.; Wang, X.; Guo, A.; Meng, X. Construction of Pumped Storage Power Stations among Cascade Reservoirs to Support the High-Quality Power Supply of the Hydro-Wind-Photovoltaic Power Generation System. *Energy Convers. Manag.* **2025**, *323*, 119239. [CrossRef]
20. Canadian Energy Regular. *Market Snapshot: Pumped-Storage Hydro—The Largest Form of Energy Storage in Canada and a Growing Contributor to Grid Reliability*; Canadian Energy Regular: Calgary, AB, Canada, 2025.
21. Li, X.; Tan, Z.; Shen, J.; Yang, J.; Fan, W.; Zhao, H.; Zhang, T. Research on the Operation Strategy of Joint Wind-Photovoltaic-Hydropower-Pumped Storage Participation in Electricity Market Based on Nash Negotiation. *J. Clean. Prod.* **2024**, *442*, 140981. [CrossRef]
22. Xiang, C.; Xu, X.; Zhang, S.; Qian, H.; Duan, Z. Current Situation of Small and Medium-Sized Pumped Storage Power Stations in Zhejiang Province. *J. Energy Storage* **2024**, *78*, 110070. [CrossRef]
23. Wang, H.; Yuan, L.; Wang, W.; Song, M. Distributionally Robust Optimization for Pumped Storage Power Station Capacity Expanding Based on Underwater Hydrogen Storage Introduction. *Energy* **2024**, *310*, 133254. [CrossRef]
24. Liu, Y.; Zhang, H.; Guo, P.; Li, C.; Wu, S. Optimal Scheduling of a Cascade Hydropower Energy Storage System for Solar and Wind Energy Accommodation. *Energies* **2024**, *17*, 2734. [CrossRef]

25. Li, Y.; Fan, Y.; Ke, X.; Huo, C.; Zhou, M.; Yang, Y.; Wang, J.; Xin, Y. Cost Recovery for Variable-Speed Pumped Storage Power Plants in the Market Environment. *Energies* **2025**, *18*, 153. [CrossRef]
26. IHA. *Pumped Storage Hydropower Capabilities and Costs*; IHA, Pumped Storage Hydropower International Forum: Paris, France, 2021; p. 24.
27. Simao, M.; Ramos, H.M. Hybrid Pumped Hydro Storage Energy Solutions towards Wind and PV Integration: Improvement on Flexibility, Reliability and Energy Costs. *Water* **2020**, *12*, 2457. [CrossRef]
28. Zhou, Y.; Zhu, Y.; Luo, Q.; Wei, Y.; Mei, Y.; Chang, F.-J. Optimizing Pumped-Storage Power Station Operation for Boosting Power Grid Absorbability to Renewable Energy. *Energy Convers. Manag.* **2024**, *299*, 117827. [CrossRef]
29. Zhou, Y.; Ning, Z.; Huang, K.; Guo, S.; Xu, C.-Y.; Chang, F.-J. Sustainable Energy Integration: Enhancing the Complementary Operation of Pumped-Storage Power and Hydropower Systems. *Renew. Sustain. Energy Rev.* **2025**, *210*, 115175. [CrossRef]
30. Wu, D.; Xiang, H.; Li, D.; Yang, J.; Liu, Z. Study on the Simulation of Electric Power Production in the Integrated Base of Hydro-Wind-Photovoltaic-Storage. *Energy Rep.* **2024**, *12*, 4617–4630. [CrossRef]
31. Global Greenfield Pumped Hydro Energy Storage Atlas—RE100—ANU. Available online: http://re100.eng.anu.edu.au/global/ (accessed on 13 June 2022).
32. Ghorbani, N.; Makian, H.; Breyer, C. A GIS-Based Method to Identify Potential Sites for Pumped Hydro Energy Storage—Case of Iran. *Energy* **2019**, *169*, 854–867. [CrossRef]
33. Joint Research Centre, Institute for Energy and Transport European Commision. *Assessment of the European Potential for Pumped Hydropower Energy Storage: A GIS Based Assessment of Pumped Hydropower Storage Potential*; Publications Office of the European Union: Luxembourg, 2013.
34. Wu, Y.; Zhang, T.; Xu, C.; Zhang, X.; Ke, Y.; Chu, H.; Xu, R. Location Selection of Seawater Pumped Hydro Storage Station in China Based on Multi-Attribute Decision Making. *Renew. Energy* **2019**, *139*, 410–425. [CrossRef]
35. Madlener, R.; Specht, J.M. An Exploratory Economic Analysis of Underground Pumped-Storage Hydro Power Plants in Abandoned Deep Coal Mines. *Energies* **2020**, *13*, 5634. [CrossRef]
36. Matos, C.R.; Carneiro, J.F.; Silva, P.P. Overview of Large-Scale Underground Energy Storage Technologies for Integration of Renewable Energies and Criteria for Reservoir Identification. *J. Energy Storage* **2019**, *21*, 241–258. [CrossRef]
37. Fan, J.; Xie, H.; Chen, J.; Jiang, D.; Li, C.; Ngaha Tiedeu, W.; Ambre, J. Preliminary Feasibility Analysis of a Hybrid Pumped-Hydro Energy Storage System Using Abandoned Coal Mine Goafs. *Appl. Energy* **2020**, *258*, 114007. [CrossRef]
38. Mongird, K.; Viswanathan, V.; Alam, J.; Vartanian, C.; Sprenkle, V.; Baxter, R. *2020 Grid Energy Storage Technology Cost and Performance Assessment*; Department of Energy: Washington, DC, USA, 2020.
39. Morabito, A.; Steimes, J.; Bontems, O.; Zohbi, G.A.; Hendrick, P. Set-up of a Pump as Turbine Use in Micro-Pumped Hydro Energy Storage: A Case of Study in Froyennes Belgium. *J. Phys. Conf. Ser.* **2017**, *813*, 012033. [CrossRef]
40. Pujades, E.; Orban, P.; Jurado, A.; Ayora, C.; Brouyère, S.; Dassargues, A. Water Chemical Evolution in Underground Pumped Storage Hydropower Plants and Induced Consequences. *Energy Procedia* **2017**, *125*, 504–510. [CrossRef]
41. Katsaprakakis, D.A.; Christakis, D.G.; Pavlopoylos, K.; Stamataki, S.; Dimitrelou, I.; Stefanakis, I.; Spanos, P. Introduction of a Wind Powered Pumped Storage System in the Isolated Insular Power System of Karpathos–Kasos. *Appl. Energy* **2012**, *97*, 38–48. [CrossRef]
42. Ioakimidis, C.S.; Genikomsakis, K.N. Integration of Seawater Pumped-Storage in the Energy System of the Island of São Miguel (Azores). *Sustainability* **2018**, *10*, 3438. [CrossRef]
43. Katsaprakakis, D.A.; Christakis, D.G. Seawater Pumped Storage Systems and Offshore Wind Parks in Islands with Low Onshore Wind Potential. A Fundamental Case Study. *Energy* **2014**, *66*, 470–486. [CrossRef]
44. Portero, U.; Velázquez, S.; Carta, J.A. Sizing of a Wind-Hydro System Using a Reversible Hydraulic Facility with Seawater. A Case Study in the Canary Islands. *Energy Convers. Manag.* **2015**, *106*, 1251–1263. [CrossRef]
45. Pradhan, A.; Marence, M.; Franca, M.J. The Adoption of Seawater Pump Storage Hydropower Systems Increases the Share of Renewable Energy Production in Small Island Developing States. *Renew. Energy* **2021**, *177*, 448–460. [CrossRef]
46. Ding, H.; Hu, Z.; Song, Y. Stochastic Optimization of the Daily Operation of Wind Farm and Pumped-Hydro-Storage Plant. *Renew. Energy* **2012**, *48*, 571–578. [CrossRef]
47. Bhayo, B.A.; Al-Kayiem, H.H.; Gilani, S.I.U.; Ismail, F.B. Power Management Optimization of Hybrid Solar Photovoltaic-Battery Integrated with Pumped-Hydro-Storage System for Standalone Electricity Generation. *Energy Convers. Manag.* **2020**, *215*, 112942. [CrossRef]
48. Yahia, Z.; Pradhan, A. Simultaneous and Sequential Stochastic Optimization Approaches for Pumped Storage Plant Scheduling with Random Breakdowns. *Energy* **2020**, *204*, 117896. [CrossRef]
49. Wild, K. Coupled Operation of a WF and PS Facility—Technico-Economic Modelling and Stochastic Optimization. Master's Thesis, University of Toronto, Toronto, ON, Canada, 2009.
50. Dilley, L.M. The Economic Feasibility of Pumped Storage Hydropower. Ph.D. Dissertation, Washington State University, Washington, DC, USA, 2016.

51. Laurent, B. Modélisation et Optimisation d'un Système de Stockage Couplé à une Production Electrique Renouvelable Intermittente. Ph.D. Thesis, Université de la Réunion, Saint-Denis, France, 2016.
52. Bakhshaei, P.; Askarzadeh, A.; Arababadi, R. Operation Optimization of a Grid-Connected Photovoltaic/Pumped Hydro Storage Considering Demand Response Program by an Improved Crow Search Algorithm. *J. Energy Storage* **2021**, *44*, 103326. [CrossRef]
53. Akbari-Dibavar, A.; Mohammadi-Ivatloo, B.; Zare, K. Optimal Stochastic Bilevel Scheduling of Pumped Hydro Storage Systems in a Pay-as-Bid Energy Market Environment. *J. Energy Storage* **2020**, *31*, 101608. [CrossRef]
54. Makhdoomi, S.; Askarzadeh, A. Optimizing Operation of a Photovoltaic/Diesel Generator Hybrid Energy System with Pumped Hydro Storage by a Modified Crow Search Algorithm. *J. Energy Storage* **2020**, *27*, 101040. [CrossRef]
55. Kuwabara, T.; Shibuya, A.; Furuta, H.; Kita, E.; Mitsuhashi, K. Design and Dynamic Response Characteristics of 400 MW Adjustable Speed Pumped Storage Unit for Ohkawachi Power Station. *IEEE Trans. Energy Convers.* **1996**, *11*, 376–384. [CrossRef]
56. Alizadeh Bidgoli, M.; Yang, W.; Ahmadian, A. DFIM versus Synchronous Machine for Variable Speed Pumped Storage Hydropower Plants: A Comparative Evaluation of Technical Performance. *Renew. Energy* **2020**, *159*, 72–86. [CrossRef]
57. Sivakumar, N.; Das, D.; Padhy, N.P. Variable Speed Operation of Reversible Pump-Turbines at Kadamparai Pumped Storage Plant—A Case Study. *Energy Convers. Manag.* **2014**, *78*, 96–104. [CrossRef]
58. Gao, C.; Yu, X.; Nan, H.; Men, C.; Zhao, P.; Cai, Q.; Fu, J. Stability and Dynamic Analysis of Doubly-Fed Variable Speed Pump Turbine Governing System Based on Hopf Bifurcation Theory. *Renew. Energy* **2021**, *175*, 568–579. [CrossRef]
59. Feng, C.; Zheng, Y.; Li, C.; Mai, Z.; Wu, W.; Chen, H. Cost Advantage of Adjustable-Speed Pumped Storage Unit for Daily Operation in Distributed Hybrid System. *Renew. Energy* **2021**, *176*, 1–10. [CrossRef]
60. EIA. Annual Energy Outlook. Available online: https://www.eia.gov/outlooks/aeo/tables_side_xls.php (accessed on 2 August 2022).
61. Ressources Naturelles Canada, Gouvernement du Canada Ressources Naturelles Canada. L'Atlas du Canada, Toporama. Available online: https://atlas.gc.ca/toporama/fr/index.html (accessed on 6 June 2022).
62. USSD Committee on Materials for Embankment Dams. *Materials for Embankments Dams*; U.S. Society on Dams: Denver, CO, USA, 2009; ISBN 978-1-884575-49-5.
63. Gouvernement du Québec. *Fiches Régionales de Sensibilisation: Les Enjeux Régionaux Des Changements Climatiques*; Gouvernement du Québec: Québec, QC, Canada, 2025; p. 115.
64. Black & Veatch. *Cost and Performance Data for Power Generation Technologies*; Black & Veatch Compagny: Overland Park, KS, USA, 2012.
65. Oladosu, G.; Sasthav, C. *Hydropower Capital and O&M Costs: An Exploration of the FERC Form 1 Data*; Oak Ridge National Laboratory: Oak Ridge, TN, USA, 2022.
66. Montmarquette, C.; Scott, I. *Taux D'actualisation Pour L'évaluation Des Investissements Publics Au Québec*; CIRANO: Montréal, QC, Canada, 2007.
67. France-Renouvelables. *Innovations Récentes Dans L'énergie Éolienne: Quelles Sont Les Améliorations Techniques?* France-Renouvelables: Paris, France, 2025.
68. Government of Canada. *Loi Sur La Tarification de La Pollution Causée Par Les Gaz à Effet de Serre: Rapport Annuel Au Parlement Pour 2020*; Environnement et Changement Climatique Canada: Gatineau, QC, Canada, 2022; p. 29.
69. Sens, L.; Neuling, U.; Kaltschmitt, M. Capital Expenditure and Levelized Cost of Electricity of Photovoltaic Plants and Wind Turbines—Development by 2050. *Renew. Energy* **2022**, *185*, 525–537. [CrossRef]
70. Wiser, R.; Bolinger, M.; Lantz, E. Assessing Wind Power Operating Costs in the United States: Results from a Survey of Wind Industry Experts. *Renew. Energy Focus* **2019**, *30*, 46–57. [CrossRef]
71. Stehly, T.; Beiter, P.; Duffy, P. *2019 Cost of Wind Energy Review*; National Renewable Energy Laboratory: Golden, CO, USA, 2020; p. 86.
72. Statistique Canada Gouvernement du Canada. Taux de Change Moyens MENSUELS en dollars Canadiens, Banque du Canada. Available online: https://www150.statcan.gc.ca/t1/tbl1/fr/tv.action?pid=3310016301 (accessed on 13 June 2022).